Nanoscale

ARTICLE

Stability and Cytotoxicity of Crystallin Amyloid Nanofibrils

Manmeet Kaur[a], Jackie Healy[a], Madhusudan Vasudevamurthy[a], Moritz Lassé[a], Ljiljana Puskar[b], Mark J. Tobin[b], Celine Valery[c], Juliet A. Gerrard*[a,d,e] and Luigi Sasso*[a,d]

Previous work has identified crystallin proteins extracted from fish eye lenses as a cheap and readily available source for the self-assembly of amyloid nanofibrils. However, before exploring potential applications, the biophysical aspects and safety of this bionanomaterial need to be assessed so as to ensure that it can be effectively and safely used. In this study, crude crystallin amyloid fibrils are shown to be stable across a wide pH range, in a number of industrially relevant solvents, at both low and high temperatures, and in the presence of proteases. Crystallin nanofibrils were compared to well characterised insulin and whey protein fibrils using Thioflavin T assays and TEM imaging. Cell cytotoxicity assays suggest no adverse impact of both mature and fragmented crystallin fibrils on cell viability of Hec-1a endometrial cells. An IR microspectroscopy study supports long-term structural integrity of crystallin nanofibrils.

1. Introduction

Amyloid protein nanofibrils (PNFs) are highly ordered, insoluble, self-assembling protein nanostructures often associated with protein misfolding diseases such as Alzheimer's disease, Parkinson's disease, Huntington's disease, and numerous others,[1-4] and also share structural similarities with spider silk,[5] curli protein,[6] bacterial inclusion bodies,[7] and in melanosomes of humans.[8]

The potential role of amyloid fibrils in the bionanotechnology sector is a topic of growing interest as PNFs offer a number of attractive features compared to the other nanostructures,[9] including ease of self-assembly synthesis, nanoscale dimensions, and their ability to act as scaffolds for functionalisation, for example through cross-linking enzymes via the amino acid side chains, [10-14] resulting in improved specific activity and stability of the immobilised enzyme.[15] Amyloid fibrils have been successfully explored for a number of potential applications or as enzyme scaffolds for biosensing, bioremediation, and other applications.[16-27] Successful examples of fibril functionalisation include cross-linking of enzymes (e.g., glucose oxidase, hydrolases) to fibrils[26,28] and cross-linking of fibrils to other surfaces (e.g., cotton, glass beads, gold particles).[29] As research continues for successfully exploiting these PNFs for a variety of nanotechnological uses[30-34] it is important to explore the feasibility of a large scale and low cost fibril production process.[35] Previous work has reported the synthesis of amyloid fibrils from crude crystallin protein mixtures, extracted from bovine lenses obtained from abattoirs.[10,35]

Fish eye lenses have also been investigated successfully for fibril manufacture, [36] due to simple extraction of the lens from the fish and ready availability of this low value by-product from the seafood industry. From a consumer perspective, fish eye lenses may be perceived as safer than bovine products in the wake of bovine spongiform encephalopathy outbreaks.[36]

To date, *in vitro* studies of amyloid fibril formation have focused mostly on fibrils generated from laboratory scale quantities of purified proteins.[37,38] The cost and time involved in generating fibrils from these proteins would hinder the large scale manufacture of amyloid fibrils for bulk nanomaterials. However, if amyloid fibrils are to be used in an industrial setting, then methods will be required for their manufacture that utilise inexpensive, crude mixtures of proteins.[39] Thus, amyloid fibrils obtained from crude extracts of marine waste proteins like crystallin proteins of fish eye lenses from *Macruronus novaezelandiae* (Hoki), offer a cheap and readily available source of fibril-forming protein material.

Many industrial enzymes are quite expensive and suffer from the serious drawback of poor stability and reusability. Additionally, for the successful application of enzymes, these catalysts need to be fully functional under, often harsh, processing conditions. Industrial parameters are often quite different from the natural environment of enzymes, with respect to temperature, pH, and organic co-solvents.[40] To address some of these issues, PNFs are ideally suited as a readily functionalised nanoscaffold for enzyme immobilisation. Successful immobilisation of industrially important enzymes onto amyloid fibrils leads to the creation of cheap and readily available protein based highly efficient matrices. Thus, it is important to consider practical issues, such as stability of these fibrils in different solutions, over a range of pH and temperature, and to understand the behaviour of these fibrils under different conditions, so as to ensure that they can be effectively used as a versatile bionanoscaffold.

In this article we present an investigation of crystallin PNF stability at a wide range of pHs, a variety of temperatures, in the presence of industrially related solvents, such as methanol (MeOH), ethanol (EtOH), isopropanol (iPrOH), and acetonitrile (ACN), on the

exposure to proteolytic enzymes such as bovine trypsin, pepsin and recombinant Proteinase K, and over long periods of storage. The Thioflavin T (ThT) assay was used to confirm the presence of fibrils under given conditions, followed by TEM imaging, to visually confirm the integrity of the nanofibrils. Crystallin nanofibrils were compared to well characterised, insulin and whey protein fibrils. The long-term structural integrity of crystallin PNFs was assessed using FTIR microspectroscopy. A cytotoxicity study was also performed to assess any potential toxicity of crystallin PNF using the Hec-1a endometrial cell line, in order to assess the biosafety of crystallin PNFs.

2. Experimental

2.1. Materials

Fish eye lenses were extracted from local *Macruronus novaezelandiae* (Hoki). The work with Hec-1a culture was kindly supported by Kenny Chitcholtan (Otago University, New Zealand). All buffers and solutions were prepared in filtered water using a Vacuubrand 2C (John Morris Scientific, Chatswood, NSW, Australia). All other chemicals and solutions, unless stated otherwise, were obtained from Sigma-Aldrich, MO.

2.2. PNF formation

Fibrils were formed using in-house methods that had been adapted from the literature. For insulin PNFs, 5.8 mg/ml of insulin (Sigma) were dissolved in 100 mM NaCl, 25 mM HCl (pH 1.6) and sterile filtered.[40] The solution was incubated at 60 °C for 22 hours. After heat incubation, the samples were cooled down in an ice bath for 10 minutes and finally stored at room temperature for 7 days to allow for fibril formation. For whey PNFs, aqueous solution of whey protein isolate (10 mg/ml) were prepared and stirred for 10 min. The pH was adjusted to 2.0 with addition of 1.0 M HCl and 0.1 M KOH using a pH probe (Denver Instrument, Bohemia, NY, USA). The solutions were left overnight at 4 °C while stirring, and then heated to 80 °C for 20-22 hours in a dry bath heater (Labnet International Inc., Woodridge, NJ, USA). After cooling for 10 min on ice, the resulting whey PNF suspensions were kept at room temperature for at least 1 week before proceeding with the experiments.[25] For crystallin PNFs, proteins were extracted from fish eye lenses and PNFs formed from this crude mixture, as previously described.[35] The presence of PNFs was confirmed using the thioflavin T (ThT) assay and TEM imaging. To study the stability of fibrils, pre-formed fibrils were subjected to the selected conditions by resuspending in an appropriate buffer/solvent. The ThT assay was used to indicate the presence of fibrils, and TEM was then used to visually confirm the presence of fibrils.

2.3. Stability experiments

For temperature stability, pre-formed fibrils were incubated at selected temperatures (-20 °C, 4 °C, 22 °C, 37 °C and 80 °C) for the time period of 24 h and aliquots were taken after 3 h, 6 h, 12 h and 24 h to perform the ThT assay at room temperature. To study the impact of pH and solvents, fibrils were incubated at room temperature in a variety of buffers and solvents: 0.1 M sodium acetate, pH 2.0, 0.1 M sodium acetate, pH 4.0, 0.1 M sodium phosphate, pH 6.0, 0.1 M sodium phosphate , pH 7.2, 0.1 M HEPES, pH 8.0, 0.1 M HEPES, pH 9.0, and sodium borate, pH 11.00; Solvents: nanopure water (H$_2$O), MeOH, EtOH, iPrOH, DMSO, and ACN, for the time period of 24 h and 3 h respectively. For the solvent study, PNFs formed in appropriate buffers were collected by

centrifugation at 10,000 rpm for 10 min, and resuspended in the test solvent. To study the impact of proteolytic enzymes, enzymes were added in an enzyme:fibril ratio of 1:20 (w/w). For trypsin and Proteinase K (PK) hydrolysis, the pH of the fibril solutions was adjusted to 7.5. For pepsin it was kept at pH 1.6. The total volume was adjusted with distilled water to yield a final protein concentration of 10 mg/ml. The fibril samples were incubated with the enzymes for 3 hours. PK and trypsin hydrolysis were terminated by adjustment to pH 1 - 2 with 1 M HCl, and pepsin digestion through adjustment to pH 7 with 1 M NaHCO$_3$. The presence and morphologies of amyloid fibrils were confirmed using the Thioflavin T (ThT) assay and TEM imaging. For ThT assay data analysis, ThT fluorescence was monitored and compared to buffer controls. Maintenance of the amyloid fibril structure in these buffers was determined by comparing ThT fluorescence to a control sample (fibril + buffer used to produce fibrils initially) and error bars represent the SD of three replicate measurements.

2.4. Thioflavin T (ThT) assay

The ThT assay was carried out according to in-house methods. ThT (2.5 mM) was made up in ThT buffer containing 50 mM Tris base, 100 mM NaCl, pH 7.5. This was filtered and stored in the dark for up to a maximum of two days. ThT fluorescence was measured using a BMG Labtech FLUOstar Optima plate reader with excitation/emission filters of 450 and 485 nm, respectively.[41] Samples had a total volume of 200 μl containing 25 μM ThT. Three replicates of each sample were measured. Where ThT values were used quantitatively, it was ensured that the pH was consistent across all samples or a normalised ThT reading with appropriate buffers or solvents was used. This ensured that any potential effects of buffer pH and ThT fluorescence could be eliminated, allowing quantification of fluorescent changes solely caused by changes in fibril quantity or morphology.

2.5. Transmission electron microscopy (TEM)

Fibril presence and morphology were assessed by TEM using negative staining with uranyl acetate (1% w/v). TEM samples were prepared using Formvar-coated copper TEM grids (200 mesh), and micrographs were taken using a Morgagni 268D TEM (FEI Company, OR, USA) operating at 80 kV and fitted with a 40 m objective aperture.

2.6. Cytotoxicity Experiments

Cytotoxicity experiments were carried out according to in-house protocols previously developed.[42]
Hec-1a cell line-Subculturing. Hec-1a cells[43] (passage 10) were cultured in Minimum Essential Medium (GIBCO®, Carlsbad, CA, USA) with GlutaMAX™ (1x), penicillin (100 U/ml), streptomycin (100 mg/ml), and 5 % fetal bovine serum (FBS). Cells were washed with sterile PBS and harvested in trypsin EDTA (1x) for 10-15 minutes. The cells were diluted 1:1 in PBS and centrifuged at 1,500 rpm for 5 min. The supernatant was replaced and the pellet taken up in 10 ml of medium. Viable cell density was determined using a hemocytometer. The Hec-1 cells were diluted to 4 x 10^8 cells/ml in media and used to seed 12-well plates (500 μl/well) for 48 hours at 37 °C (80% confluence).
Treatment. Medium was removed from the seeded Hec-1a cells prior to treatment. Each treatment consisted of 500 μl of sample protein at ~10 mg/ml in PBS (final concentration ~5 mg/ml) mixed with 500 μl of minimal essential medium (MEM) respectively. Cells were incubated at 37 °C for 24 hours. At least three replicates for

each condition were measured. The used control was cells + medium + buffer (PBS). Further, to assess if cells use protein as a nutrient source, cells were pre-incubated in the absence of fetal bovine serum (FBS) overnight to starve them prior to the addition of treatments.
Crystal violet assay. The medium of the treated cells was discarded and 300 μl of crystal violet[44] stain was added to each of the 12 wells. After staining for 15 minutes the excess stain was thoroughly washed off with distilled water until completely removed. The plates were dried before re-solubilising the stained cells in 1 ml of 2 % SDS solution per well. After solubilising the dye-containing cells, the absorbance of the solutions was measured at 570 nm on a Labtech FLUOstar OPTIMA plate reader (BMG Labtech GmbH, Offenburg, Gemany).

2.7. Infrared (IR) microspectroscopy

After storage in the original solvent for long periods of time (up to 37 months), the fibril samples were washed in water 3 times by centrifugation (10000 rpm for 10 min each wash) and concentrated to a final concentration > 100 mg/ml. Infrared microspectroscopy was carried out at the Australian Synchrotron, using the IR Microspectroscopy (IRM) beamline which combines a Bruker V80v Fourier transform infrared (FTIR) spectrometer and a Hyperion 2000 IR microscope with a liquid nitrogen cooled narrow-band mercury cadmium telluride (MCT) detector. A small amount of washed fibril sample was placed between two diamond windows of a ThermoFisher (Waltham, MA, USA) micro compression cell and the data collected in transmission mode with a microscope aperture defining a measurement area of 5 μm x 5 μm on the sample. The supernatant from the last wash was used as the background. Each spectrum was collected in the mid-infrared spectral range (4000–700 cm^{-1}) with 64 co-added scans and spectral resolution of 4 cm^{-1}. Bruker OPUS 6.5 software was used for data collection and Bruker OPUS 7.2 for the spectral analysis and for the calculation of the second derivative using a 9 to 15 point Savitzky-Golay filter.

3. Results and discussion

3.1. Effect of proteases on PNFs

One of the hallmarks of amyloid fibrils is their high resistance to proteases compared to the natively folded protein.[40,44-46] To assess the extent of fibril digestion, proteolytic enzymes such as bovine trypsin, pepsin and recombinant Proteinase K were used. Several *in vitro* digestibility assays using pepsin and trypsin have been conducted as they are physiologically relevant proteases.[47-49] Proteinase K is a broad-spectrum and highly active protease that has been used extensively to characterise the protease resistance of disease-related amyloid fibrils.[50,51] Digestion reactions of fibrils were carried out in appropriate buffers and the degree of fibril digestion was assessed after 3 hours by the ThT fluorescence decrease and TEM analysis.
The ThT assay was selected as it is well accepted as an indicator of the presence of amyloid fibrils.[41,52-54] Upon its incorporation into amyloid fibrils, ThT exhibits a considerable increase in the fluorescence intensity; however, the interaction mechanism between ThT and amyloid fibrils remains to be elucidated.[55,56] As the ThT assay is known to be sensitive to pH and viscosity, [57,58] care was taken to have appropriate ThT control measurements in each of the buffers or solvents used for experiments (see ESI Fig. S1 and S2†). ThT fluorescence during digestion was monitored and compared to buffer controls.
Insulin PNFs, used as a well characterised standard for comparison, proved to be the most resistant fibrils to proteolysis, followed by

crystallin PNFs (in presence of all three proteases), as indicated by a constant ThT fluorescence over the entire duration of the experiment (see Fig. 1A). Both insulin and crystallin PNFs displayed high resistance towards protease digestion. However, whey PNFs exhibited different digestion patterns towards different proteases, a result already confirmed by the available literature on this specific PNF type.[59-60]
TEM micrographs of fibrils were obtained following the 3 hour digestion in order to assess the change of morphology of the fibrils before and after treatment. Although some enzymatic digestion was present in all samples, there were still considerable amounts of fibrils present after the 3 hour digestion by pepsin, trypsin and even by Proteinase K (see Fig. 1B), consistent with observations from ThT fluorescence, and indicating partial digestion of the whey PNFs (also shown in Fig. 1B-h), whereas there was still a high fluorescence after 3 hours of trypsin and pepsin digestion of the whey PNFs. The general pattern is a slightly higher resistance towards pepsin and trypsin digestion than towards Proteinase K digestion.

3.2. Effect of solvents on PNFs

This part of the study focused on PNF's resistance to common biological buffers and solvents used especially in cleanroom-based microfabrication: MeOH, EtOH, DMSO, iPrOH, ACN, and H$_2$O. After a washing step (3 times in nanopure water) fibrils were resuspended in the test solvent and a ThT assay was then carried out on these samples after a 3 hour incubation at room temperature. The influence of different solvents on each of the PNFs used was determined by comparing the decrease in ThT fluorescence to the control sample (fibrils resuspended in the buffer initially used to produce them).
For all three types of PNFs, a significant decrease in ThT fluorescence was seen in the samples resuspended in DMSO and ACN, with ACN-incubation exhibiting the largest decrease, as depicted in Fig. 2A. In the presence of MeOH, EtOH, iPrOH and H$_2$O, all three types of PNFs exhibited high ThT fluorescence indicating fibril stability in the presence of these solvents. However, in comparison to insulin and crystallin PNFs, whey PNFs in the presence of methanol and ethanol showed a considerable and slight, respectively, decrease in ThT fluorescence, which is hypothesized to be due to the fibrils degrading or solubilising.[61] From the obtained ThT fluorescence readings, in all the other solvents used, except DMSO and ACN, crystallin PNFs exhibited maximum stability, followed by insulin PNFs and whey PNFs, without any remarkable difference in ThT fluorescence after 3 h of incubation. The high decrease in ThT fluorescence for the samples resuspended in DMSO and ACN is expected, since organic solvents, mainly polar aprotic solvents including DMSO and ACN, have previously been shown to dissolve amyloid fibrils.[62]
To validate the observed changes in ThT fluorescence, TEM analysis was carried out to confirm the presence or absence of fibrils in each of the samples (see Fig. 2B). For all the three types of PNFs used, resuspension in water yielded amyloid fibrils typical of a control fibril preparation indicating that centrifugation and resuspension procedures had not damaged the fibrils, which appeared unchanged (g,n,u compared to a,h,o respectively). TEM images for the samples of crystallin, insulin and whey PNFs resuspended in EtOH, iPrOH, and MeOH also show the presence of clear fibrils (Fig. 2B). However, in the case of the methanol sample for whey PNFs there is a change in morphology of the fibrils.
In the case of ACN and DMSO, for insulin and whey PNFs (Fig. 2B-e,f;l,m) no clear fibril morphology can be observed, which could be due to fibrils dissolving, in agreement with the low ThT fluorescence

readings. However, for the crystallin PNFs incubated in DMSO and ACN, TEM images suggest the presence of fibrils with slightly different morphologies (Fig. 2B-s,t). The results obtained are in agreement to similar study done on crystallin PNFs by Domigan *et al.* 2013,[25] who investigated the effect of ACN by resuspending fibrils in 50 % ACN. Loss of β-sheet content in amyloid aggregates in presence of DMSO and ACN has been reported previously.[63] The significant decrease in ThT fluorescence and lack of clear fibril morphology for whey and insulin fibrils dissolved in DMSO and ACN could be due to inhibition of hydrophobically driven association, leading to a lack in extensive self-assembly.[64] Studies have revealed[65] that pure DMSO can cause complete loss of β-sheet structure as it competes with protein carbonyl groups for hydrogen bonding to protein amine groups, leading to destabilisation of secondary structures. In the case of whey PNFs, TEM images obtained indicated that, in most of the solvents, fibrils are present but different morphologies were observed, illustrating fibril rearrangement in different solvent environments.

Comparing the stability of crystallin amyloid fibrils with diphenylalanine (FF) nanotubes in various solvents,[66] it can be confirmed that crystallin amyloid fibrils are significantly more stable in solution than FF nanotubes, and therefore could be a more appropriate choice for applications where solvent contact is involved, such as biosensing. This high stability of crystallin amyloid fibrils could be attributed to the presence of a high proportion of interstrand bridges on the crystallins as compared to other proteins.[67-69] In general, this comparative study of PNFs obtained from different sources has revealed that crystallin PNFs obtained from crude proteins obtained from fish eye lenses not only offer a cheap and readily available source for nanofibril production, but also provide fibrils with better stability in a diverse range of solvents compared to PNFs derived from other protein sources.

3.3. Effect of pH and temperature on PNFs

Previous studies have characterised the effect of pH on fibril self-assembly.[70-73] However, not much literature is available on the long term stability of PNFs at different pH values post-assembly. To study the impact of pH on pre-formed PNFs, a wide range of buffers at both acidic and alkaline pH values were selected. To test the effect of biological pH, 100 mM phosphate buffer at pH 7.4, was selected as a commonly used biological buffer solution.

Fibril stability differed at varying pH, with crystallin PNFs displaying great stability at all pHs tested. For all PNFs, no observable decrease in ThT fluorescence was observed when fibrils were resuspended in solutions with pH values between pH 2.0 and 8.0. (Fig. 3A). For whey and insulin PNFs between pH 9.0 and 11.0, a considerable decrease in ThT fluorescence was observed, indicating fibril solubilisation. The results obtained for insulin PNFs (grown under similar pH conditions) are consistent with recent findings[72] demonstrating the dissociation of insulin amyloid fibrils in this pH range using fibril recovery after centrifugal sedimentation.

The ThT fluorescence data were supported by examination of the fibrils in each of the buffers by TEM (see ESI Fig. S3†). In agreement with the ThT fluorescence assay described above, abundant fibrils were observed between pH 2.0 and pH 8.0 for all PNFs. For whey and insulin PNFs, fewer fibrils were present at pH 9.0, and no clear fibrils were detected at pH 11.0, confirming their dissociation in this pH range, whereas crystallin PNFs retained morphology over the entire pH range.

Although for insulin and whey PNFs no significant decrease in ThT fluorescence was observed for fibrils at below pH 8.0, fibrils at pH 6.0 and 8.0 were morphologically distinct from those at pH 2.0 and 4.0. For insulin fibrils, fibrils at pH 6.0 and 8.0 appear short and

discrete whereas for whey fibrils, fibrils at elevated pH values appear aggregated and clumped together (ESI Fig. S3†).

The observation of slightly different morphologies at high pH values was not an unexpected result, as morphological differences have been seen previously with elevated pH in fibrils formed from bovine insulin[74] and from crude bovine crystallins.[75]

To study the impact of temperature on pre-formed PNFs, fibrils in the respective buffers used to produce them were incubated at selected temperatures for 24 h. The range of temperatures was selected according to the optimal temperature range of industrial enzymes, considering the application of protein fibrils as versatile enzyme nanoscaffolds. After a 24 h incubation at the selected temperatures, no significant decreases in ThT fluorescence was seen for any of the fibrils. However, for insulin and whey PNFs a slight decrease in ThT fluorescence was observed (Fig. 3B). In agreement with the high ThT fluorescence readings, TEM images of the crystallin fibril samples at all the given temperatures confirmed the presence of fibrils with no major morphological differences as compared to the control (ESI Fig. S4†). A similar trend was seen for TEM images of samples taken for insulin and whey PNFs, all showing clear fibrils.

3.4. Effects of crystallin PNFs on Hec-1a cell proliferation

For toxicity studies, cell viability was measured in the presence and absence of crude crystallin proteins, mature amyloid fibrils, and sonicated (fragmented) fibrils (Fig. 4A). The crystal violet assay, a method of similar accuracy as WST (water soluble Tetrazolium salts) assays,[43,76] was performed to assess the potential toxicity of crystallin amyloid fibrils. Hec-1a cells were incubated with 10 mg/ml concentration of the crude protein, mature fibrils and sonicated fibrils, and the number of viable cells measured by the binding of crystal violet after 24 and 48 h. After 24 h as compared to the control, no significant difference in the number of viable cells exposed to any of the given treatments was observed (see Fig. 4B). Even after 48 h incubation, no significant changes were seen. A further study was undertaken to assess if there is any interaction between the cell membrane and the proteins. In comparison to the previous experiment there is a marked increase of cell viability in the presence of fibrils after 48 h incubation (as depicted in Fig. 4C). This indicates that the cells can metabolise the fibrillar protein, although the contribution of non-fibrillar protein components could contribute to the observed effect. The control (buffer + media) show that the buffer conditions do not change the cell viability. 10 % DMSO is toxic to cells and was therefore used as a positive control. The no-cell control also did not show any sign of viability, demonstrating that no contamination was present.

Despite of extensive studies in recent years,[77-79] the identity of the culprits of cytotoxicity associated with amyloidosis still remains unclear.[80] Although non-fibrillar oligomers are the main focus of attention, significant amount of studies have reported that mature amyloid fibrils can also produce a cytotoxic effect.[81-84] However, recent studies have shown that some amyloid fibrils formed from non-toxic protein sources are non-toxic, suggesting that there is a combined effect of source protein, physicochemical properties of PNFs, and cell line physiology, that affects cell viability.[23, 42]

Our results suggest that Hec-1a cells are not adversely affected by the presence of crystallin amyloid fibrils at the studied concentration. There was also no indication that fragmented (sonicated) fibrils decreased cell viability, in contrast to literature reports.[85] Instead, the *in vitro* studies suggest that the cells can perhaps utilise the fibrillar proteins as a source of nutrients, although the contribution of non-fibrillar protein components requires further investigation. As the potential interaction of fibrils with cell membranes could differ,[85]

further studies may be required using different cell lines with altered compositions of cellular membranes.

3.5. Long-term storage stability

The long term stability of the crystallin amyloid fold was investigated by infrared microspectroscopy (IRM). The analysis was focused on amide I vibrations (1600-1700 cm^{-1}), which are commonly used as conformational markers for peptides and proteins.[86] Amide I vibrations mainly arise from stretching vibrational modes of the backbone carbonyl groups and correspond to different strengths/types of hydrogen bonds in which the backbone carbonyl groups are involved. They can hence be assigned to specific secondary structures.[86]

IRM spectra were collected on crystallin fibrils aged for 2 to 37 months in water at room temperature. These were compared to IRM spectra collected for recently formed fibrils kept under the same conditions (less than a month old). IRM spectra were consistent within the same sample (data not shown). Representative amide I vibrations are here shown as a function of the aging time together with the corresponding second derivatives (Fig. 5, left and right panel respectively). Independent of the aging time, the amide I region exhibited two well-defined infrared absorption peaks at around 1620 cm^{-1} and 1690 cm^{-1} for all the samples, as for the recently formed fibrils (Fig. 5, Table 1). In accordance with the literature, this pair of absorption peaks was assigned to extended antiparallel β-sheet networks, which are a hallmark of the amyloid fibril fold.[50,86,87]

Less defined vibrations could be detected at around 1650 cm^{-1} and 1670-1680 cm^{-1} from the second derivative spectra (Table 1). These were assigned to respectively random coil and turn secondary structures.[88] The variation of the type of turn from one sample to another (1 or 2 absorption peaks) is likely due to the variation in content of the types of crystallins.[88] Similar IR amide I vibrations including antiparallel β-sheet, random coil and turn, were previously reported for amyloid fibrils generated from a γD-crystallin domain.[89] Taken together, the IRM results show that the crystallin fibrils conserve the same conformational features for up to 37 months when kept in water at room temperature. These features are typical of the amyloid fold and consistent with previous conformational characterizations of γD-crystallin amyloid fibrils.

Conclusions

Crude crystallin proteins extracted from fish eye lenses have been previously identified as an economically viable source of PNFs, allowing for amyloid fibril production in large quantities at a low cost. This paper has investigated the suitability of this material as a bionanoscaffold, specifically in terms of stability under a variety of parameters. Crystallin PNFs were shown to be stable across a wide pH range, in a number of industrially relevant solvents, at both low and high temperatures, and in the presence of proteases. A comparative study, including insulin and whey nanofibrils suggests that crystallin PNFs obtained from cheap and readily available protein source, offer similar and often improved stability properties. No evidence of cytotoxicity of crystallin PNFs has been found by preliminary cytotoxicity assays using Hec-1a cells. An IR microspectroscopy study illustrates the long-term (up to 3 years) structural integrity of crystallin nanofibrils. This study supports the use of crystallin PNFs as nanomaterials, particularly in applications such as biosensing and enzyme immobilisation, which require prolonged solvent contact and stability over a wide range of pHs and temperatures. Due to their excellent aspect ratio and stability, crystallin amyloid fibrils show promise as a novel nanosupport for the creation of functional bionanomaterials, for example, active surface coatings for the production of fine chemicals, chemical detoxification, or biosensing.

Notes and reference

^{a} Biomolecular Interaction Centre and School of Biological Sciences, University of Canterbury, Christchurch 8140, New Zealand
^{b} Australian Synchrotron, Clayton VIC 3168, Australia
^{c} School of Medical Sciences and Health Innovations Research Institute, RMIT University, Bundoora VIC 3083, Australia
^{d} MacDiarmid Institute for Advanced Materials and Nanotechnology, Wellington 6140, New Zealand. E-mail: luigi.sasso@canterbury.ac.nz
^{e} Callaghan Innovation Research Ltd, Lower Hutt 5040, New Zealand.
* luigi.sasso@canterbury.ac.nz and/or juliet.gerrard@canterbury.ac.nz

† Electronic Supplementary Information (ESI) available: ThT fluorescence graphs of buffers and solvents used for normalising ThT fluorescence of PNFs in the experiments (Fig. S1 and S2). Representative TEM images of fibrils over a wide range of pH and at variety of temperatures (Fig. S3 and S4). IR spectra of the amide fingerprinting region, including baseline (Fig. S5). See DOI: 10.1039/b000000x/

1. Pedersen, J.S.; Otzen, D.E. *Prot. Sci.* 2000, **17**, 2–10
2. Sipe, J.D.; Cohen, A.S. *J. Struct. Biol.* 2000, **130**, 88-98
3. Gras SL. *Aust. J. Chem.* 2007, **60**, 333–342
4. Chiti, F.; Dobson, C.M. *Annu. Rev. Biochem.* 2006, **75**, 333–366
5. Kenney, J.M; Knight, D.; Wise, M.J.; Vollrath, F. *Eur. J. Biochem.* 2002, **269**, 4159-4163
6. Chapman, M.R.; Robinson, L.S.; Pinkner, J.S.; Roth, R.; Heuser. J.; Hammar, M.; Normark, S.; Hultgren, S.J. *Science.* 2002, **295**, 851–855
7. Wang, L. *Prion* 2009, **3**, 139-145
8. Fowler, D.M.; Koulov, A.V.; Alory-Jost, C.; Marks, M.S.; Balch, W.E.; Kelly, J.W. *PLoS Biol.* 2005, **4**, 100-107
9. Zganec, M.; Zerovnik, E. *Biochim. Biophys. Acta* 2014, **1840**, 2944-2952
10. Waterhouse, S.H.; Gerrard, J.A. *Aust. J. Chem.* 2004, **57**, 519–523
11. Cherny, I.; Gazit, E. *Angew. Chem. Int. Ed.* 2008, **47**, 4062–4069
12. Gras, S.; Tickler, A.; Squires, A.; Devlin, G.; Horton, M.; Dobson, C.; MacPhee, C. 2008, **29**, 1553– 1562
13. Gras, S.L. *Adv. Chem. Eng.* 2009, **35**, 161–209
14. Mankar, S.; Anoop A.; Sen, S.; Maji, S.K. *Nano Rev.* 2011, **2**, 6032
15. Lee, G.; Joo, H.; Lee, J. *Mol. Catal. B Enzym.* 2008, **54**, 116-121
16. Scheibel, T.; Parthasarathy, R.; Sawick, G.; Lin, X.M.; Jaeger, H.; Lindquist, S.L. *Proc. Natl. Acad. Sci. U.S.A.* 2003, **100**, 4527–4532
17. Tang, Q.; Solin, N.; Lu, J.; Inganas, O. *Chem. Commun.* 2010, **46**, 4157–4159
18. Li, C.; Adamcik, J.; Mezzenga, R. *Nature Nanotech.* 2012, **7**, 421-427
19. Bolisetty, S.; Adamcik, J.; Heier, J.; Mezzenga, R. *Adv. Funct. Mat.* 2012, **22**, 3424-3428
20. Reynolds, N.P.; Styan, K.E.; Easton, C.D.; Li, Y.; Waddington, L.; Lara, C.; Forsythe, J.S.; Mezzenga, R.; Hartley, P.G.; Muir, B.W. *Biomacromol.* 2013, **14**, 2305-2316
21. Li, C.; Bolisetty, S.; Mezzenga, R. *Adv. Mat.* 2013, **25**, 3694-3700
22. Li, C.; Born, A.-K.; Schweizer, T.; Zenobi-Wong, M.; Cerruti, M.; Mezzenga, R. *Adv. Mat.* 2014, **26**, 3207-3212
23. Bolisetty, S.; Boddupalli, C.S.; Handschin, S.; Chaitanya, K.; Adamcik, J.; Saito, Y.; Manz, M.G., Mezzenga, R. *Biomacromol.* 2014, **15**, 2793-2799
24. Rao, S.P.; Meade, S.J; Healy, J.P.; Sutton, K.H.; Larsen, N.G.; Staiger, M.P.; Gerrard, J.A. *Biotechnol. Prog.* 2012, **28**, 248–256

25. Domigan, L.; Andersen, K.B.; Sasso, L.; Dimaki, M.; Svendsen, W.E.; Gerrard, J.A.; Castillo-Leon, J. *Electrophoresis* 2013, **34**, 1105–1112

26. Raynes, J.K.; Pearce, F.G.; Meade, S.J.; Gerrard, J.A. *Biotechnol. Prog.* 2011, **27**, 360–367

27. Hauser, C.; Maurer-Strohb, S.; Martins, I.C. *Chem. Soc. Rev.* 2014, **43**, 5326

28. Pilkington, S.M.; Roberts, S.J.; Meade, S.J.; Gerrard, J.A. *Biotechnol. Prog.* 2010, **26**, 93–100

29. Kim, S.; Bae, S.Y.; Lee, B.Y.; Kim, T.D. *Anal. Biochem.* 2012, **421**, 776–778

30. Sasso, L.; Suie, S.; Domigan, L.; Healy, J.; Nock, V.; Williams, M.A.; Gerrard, J.A. *Nanoscale.* 2014, **6**, 1629-1634

31. Gazit, E. *Chem. Soc. Rev.* 2007, **36**, 1263–1269

32. Gras, S.L. *Adv. Powder. Tech.* 2007, **18**, 699–705

33. Hamedi, M.; Herland, A.; Karlsson, R.H.; Inganas, O. *Nano. Lett.* 2008, **8**, 1736–1740

34. Li, C.; Mezzenga, R. *Nanoscale.* 2013, **5**, 6207-18

35. Garvey, M.; Gras, S.L.; Meehan, S.; Meade, S.J.; Carver, J.A.; Gerrard, J. A. *Int. J. Nanotechnol.* 2009, **6**, 258–273

36. Healy, J.; Wong, K.; Sawyer, E.B.; Roux, C.; Domigan, L.; Gras, S.L.; Sunde, M.; Larsen, N.G.; Gerrard, J.A.; Vasudevamurthy, M. *Biopolymers.* 2012, **97**, 595–606

37. Murphy, R.M. *Biochim. Biophys. Acta.* 2007, **1768**, 1923-1934

38. Munishkina, L.A.; Fink, A.L. *Biochim. Biophys. Acta.* 2007, **1768**, 1862-1885

39. Liese, A.; Hilterhaus, L. *Chem. Soc. Rev.* 2013, **42**, 6236

40. Mishra, R.S.; Basu, S.; Gu, Y.; Luo, X.; Zou, W.Q.; Mishra, R.; Li ,R.; Chen, S.G.; Gambetti, P.; Fujioko, H.; Singh, N. *J. Neurosci.* 2004, **24**, 11280–11290

41. LeVine, III H. *Prot. Sci.* 1993, **2**, 404–410

42. Lassé, M. Does the Protein Aggregation State Affect the Digestibility and Safety of Foods?, *PhD Thesis*, University of Canterbury, 2013

43. Kamat, A.A.; Meritt, W.M.; Coffey, D.; Lin, G.Y.; Patel, P.R.; Broaddus, R.; Nugent, E.; Han, L.Y.; Landen, C.N. Jr.; Spanuth, W.A.; Lu, C.; Coleman, R.L.; Gershenson, D.M.; Sood, A.K. *Clin. Cancer Res.* 2007, **13**, 7487-7495

44. Ishiyama, M.; Tominaga, H.; Shiga, M.; Sasamoto, K. *Biol. Phar. Bull.* 1996, **19**, 1518

45. Nordstedt, C.; Näslund, J.; Tjernberg, L.O.; Karlström, A.R.; Thyberg, J.; Terenius, L. *J. Biol. Chem.* 1994, **269**, 30773–30776

46. Selvaggini, C.; Gioia, L.; Cantu, L.; Ghibaudi, E.; Diomede, L.; Passerini, F.; Forloni ,G.; Bugiani, O.; Tagliavini, F.; Salmona, M. *Biochem. Biophys. Res. Commun.* 1993, **194**, 1380–1386

47. DeBaun, R.M.; Connors, W.M. *J. Agric. Food Chem.* 1954, **2**, 524-526

48. Thresher, W.C.; Swaisgood, H.E; Catignani, G.L. *Plant Food. Hum. Nutr.* 1989, **39**, 59-65

49. Thomas, K.; Aalbers, M.; Bannon, G.A.; Bartels, M.; Dearman, R.J.; Esdaile, D.J.; Fu, T.J.; Glatt, C.M.; Hadfield, N.; Hatzos, C.; Hefle, S.L; Heylings, J.R.; Goodman, R.E.; Henry, B.; Herouet, C.; Holsapple, M.; Ladics, G.S.; Landry, T.D.; MacIntosh, S.C.; Rice, E.A.; Privalle, L.S.; Steiner, H.Y.; Teshima, R.; Van Ree, R.; Woolhiser, M.; Zawodny, J. *Regul. Toxicol. Pharm.* 2004, **39**, 57-98

50. Watts, J.C.; Stöhr, J.; Bhardwaj, S.; Wille, H.; Oehler, A.; De-Armond, S.J.; Giles, K.; Prusiner ,S.B. *PLoS Pathog.* 2011, DOI: 10.1371/journal.ppat.1002382

51. Colby, D.W.; Wain, R.; Baskakov, IV.; Legname, G.; Palmer, C.G. *PLoS Pathog.* 2010, DOI: 10.1371/journal.ppat.1000736

52. Ebeling, W.; Hennrich, N.; Klockow, M.; Metz, H.; Orth, H.D.; Lang, H. *Eur. J. Biochem.* 1974, **47**, 91–97

53. Kisilevsky, R.; Fraser, P.E. *Critic. Rev. Biochem. Mol. Biol.* 1997, 32, 361-404

54. Nilsson, M.R. *Methods*, 2004, **34**, 151-160

55. Biancalana, M.; Koide, S. *Biochim. Biophys. Acta.* 2010, **1804**, 1405-1412

56. Khurana, R.; Coleman, C,; Ionescu-Zanetti, C.; Carter, S.A.; Krishna, V.; Gorver, R.K.; Roy, R.; Singh, S. *J. Struct. Biol.* 2005, **151**, 229-38

57. Sabaté, R.; Lascu, I.; Saupe, S.J. *J. Struct. Biol.* 2002, **162**,387–396

58. Sulatskaya, A.I.; Maskevich, A.; Kuznetsova, I.; Uversky, V.; Turoverov, K. *PLoS One.* 2010, DOI: 10.1371/journal.pone.0015385

59. Bateman, L.; Ye, A.; Singh, H. *J. Agric. Food Chem.* 2010, **58**, 9800-9808

60. Peram, M.R.; Loveday, S.M.; Ye, A.; Singh, H. *J. Dairy Sci.* 2013, **96**, 63-74

61. Jordens, S; Adamcik, J.; Amar-Yuli, I.; Mezzenga, R. *Biomacromol.* 2011, **12**, 187-193

62. Hirota-Nakaoka, N.; Hasegawa, K.; Naiki, H.; Goto, Y. *J. Biochem.* 2003, **134**,159–164

63. Shen, C.L.; Murphy, R.M. *Biophys. J.* 1995, **69**, 640-651

64. Snyder, S.W.; Ladror, U.S.; Wade, W.S.; Wang, G.T.; Barrett, L.W.; Matayoshi, E.D.; Huffaker, H.J.; Krafft, G.A.; Holzman, T.F. *Biophys. J.* 1994, **67**, 1216–1228

65. Jackson, M.; Mantsch, H.H. *Biochim. Biophys. Acta.* 1991, 1078, 231–235

66. Andersen, K.B.; Castillo-León, J.; Hedstrom, M.; Svendsen, W.E. *Nanoscale* 2011, **3**, 994–998

67. Sarakatsannis, J.N.; Duan, Y. *Proteins* 2005, **60**, 732-739

68. Donald, J.E.; Kulp, D.W.; Degrado, W.F. *Proteins* 2011, **79**, 898-915

69. Mahendiran, K.; Elie, C.; Nebel, J.C.; Ryan, A.; Pierscionek, B.K. *Sci. Rep.* 2014, 2045-2322

70. Nielsen, L.; Khurana, R.; Coats, A.; Frokjaer, S.; Brange, J.; Vyas, S.; Uversky, N.V.; Fink, A,L. *Biochem.* 2001, **40**, 6036-6046

71. Schmittschmitt, J.P.; Scholtz, J.M. *Prot. Sci.* 2003, **12**, 2374–2378

72. Shammas, S.L.; Tuomas, P.; Knowles, J.; Baldwin, A.J.; Cait, E.; MacPhee, C.; Welland, M.E.; Dobson, C.M.; Devlin, G.L. *Biophys. J.* 2011, **100**, 2783-2791

73. Loveday, S.M.; Wang, X.L.; Rao, M.A.; Anema, S.G.; Singh, H. *J. Agric. Food Chem.* 2011, **15**, 8467-8474

74. Rao, S. Amyloid fibrils in bionanomaterials, *PhD Thesis*, University of Canterbury, 2008

75. Pilkington, S. Incorporating glucose oxidase activity into amyloid fibrils, *Master's Thesis*, University of Canterbury, 2009

76. Flick, D.A.; Gifford, G.E. *J. Immunol. Methods.* 1984, **68**, 167–175

77. Kayed, R.; Head, E.; Thompson, J.L.; McIntire, T.M.; Milton, S.C.; Cotman, C.W.; Glabe, C.G. *Science* 2003, **300**, 486-489

78. Martins, I.C.; Kuperstein, I.; Wilkinson, H.; Maes, E.; Vanbrabant, M.; Jonckheere, W.; Van Gelder, P.; Hartmann, D.; De-Strooper, B.; Schymkowitz, J.; Rousseau, F. *EMBO. J.* 2008, **27**, 224-233

79. Shankar, G.M.; Li, S.; Mehta, T.H.; Garcia-Munoz, A.; Shepardson, N.E.; Smith, I.; Brett, F.M.; Farell, M.A.; Rowan, M.J.; Lemere, C.A.; Regan, C.M.; Walsh, D.M.; Sabatini, B.L.; Selkoe, D.J. *Nat. Med.* 2008, **14**, 837-842

80. Eisenberg, D.; Jucker, M. *Cell* 2012, **148**, 1188-1203

81. Malisauskas, D.; Darinskas, A.; Zamotin, V.; Gharibyan, A.; Kostanyan, I.A.; Morozova- Roche, L.A. *Biochem.* 2006, 71, 505-512

82. Campioni, S.; Mannini, B.; Zampagni, M.; Pensalfini, A.; Parrini, C.; Evangelisti, E. *Nat. Chem. Biol.* 2010, **6**, 140-147

83. Meyer-Luehmann, M.; Spires-Jones, T.L.; Prada, C.; Garcia-Alloza, M.; De Calignon, A.; Rozkalne, A. *Nature* 2008, **451**, 720-724

84. Engel, M.F.; Khemtemourian, L.; Kliejer, C.C.; Meeldijik, H.J.; Jacobs, J.; Verkleij, A. J. *Proc. Natl. Acad. Sci. U.S.A.* 2008, **105**, 6033-6038

85. Xue, W.F.; Hellewell, A.L.; Gosal, W.S.; Homans, S.W.; Hewitt, E.W.; Radford, S.E. *J. Biol. Chem.* 2009, 284, 34272-34282

86. Barth, A. *Biochim. Biophys. Acta.* 2007, **1767**, 1073-101

87. Van Grondelle, W.; Lecomte, S.; Lopez-Iglesias, C.; Manero, J.M.; Cherif-Cheikh, R.; Paternostre, M.; Valéry, C. *Faraday Disc.* 2013,166, 163-80

88. Garvey, M.; Gras, S.L.; Meehan, S.; Meade, S.J.; Carver, J.A.; Gerrard, J.A. *Int. J. Nanotechnol.* 2009, **6**, 258-273

89. Moran, S.D.; Woys, A.M.; Buchanan, L.E.; Bixby, E.; Decatur, S.M.; Zanni, M.T. *Proc. Natl. Acad. Sci. U.S.A.* 2012, **109**, 3329-3334
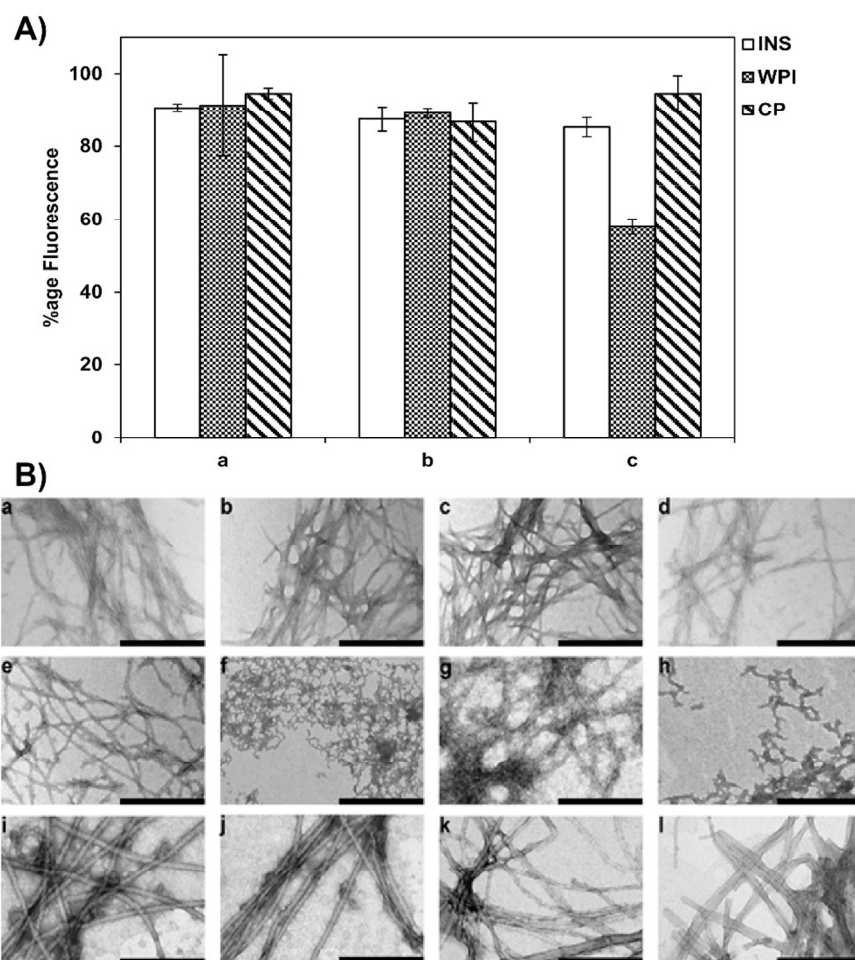
Figure 1. (A) ThT fluorescence of insulin (INS), whey protein (WPI) and crystalline (CP) PNFs in presence of proteolytic enzymes, after 3h incubation at room temperature. ThT fluorescence is represented as % decrease in fluorescence compared to the control sample. For data analysis, the data was normalised to a control sample. Samples from left to right: (a) trypsin, (b) pepsin, and (c) Proteinase K. Error bars represent the SD of three replicates. (B) Representative TEM images of PNFs after incubation with proteolytic enzymes. Row 1: insulin PNFs - (a) control, (b) trypsin, (c) pepsin, and (d) Proteinase K. Row 2: whey PNFs - (e) control, (f) trypsin, (g) pepsin, and (h) Proteinase K. Row 3: crystallin PNFs - (i) control, (j) trypsin, (k) pepsin, and (l) Proteinase K. Scale bar is 100 nm
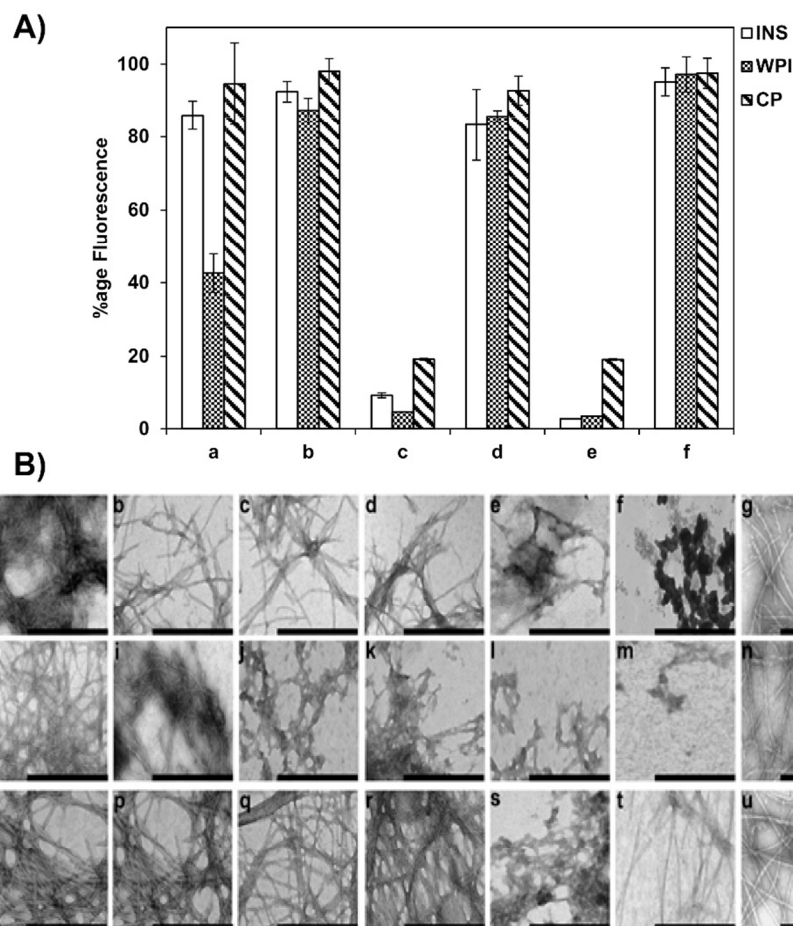
A)

B)

Figure 2. A) ThT fluorescence of insulin (INS), whey (WPI) and crystallin (CP) PNFs resuspended in various solvents, after 3 h incubation. ThT fluorescence is represented as % decrease in fluorescence compared to the control sample. Samples from left to right: (a) MeOH, (b) EtOH, (c) DMSO, (d) iPrOH, (e) ACN, and (f) H_2O. Fluorescence values have all had the appropriate control value subtracted. Error bars represent the SD of three replicates. B) Representative TEM images of fibrils resuspended in solvents. Row 1: insulin PNFs - (a) Control, (b) MeOH, (c) EtOH, (d) iPrOH, (e) DMSO, (f) ACN, and (g) H_2O. Row 2: whey PNFs - (h) Control, (i) MeOH, (j) EtOH, (k) iPrOH, (l) DMSO, (m) ACN, and (n) H_2O. Row 3: crystallin PNFs - (o) Control, (p) MeOH, (q) EtOH, (r) iPrOH, (s) DMSO, (t) ACN, and (u) H_2O. Scale bar is 100 nm
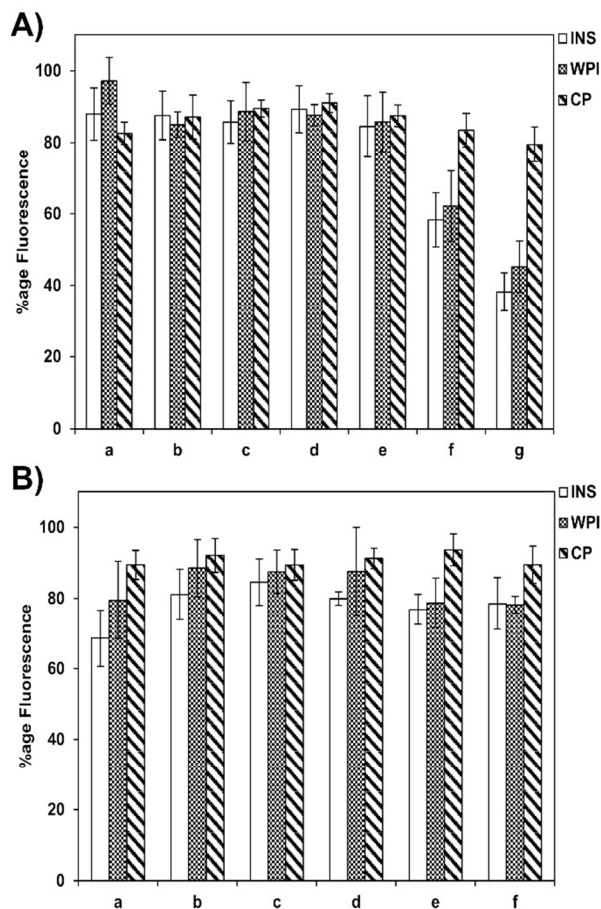
Figure 3. A) ThT fluorescence of insulin (INS), whey (WPI) and crystallin (CP) PNFs resuspended in buffers at different pH values, after 24 h incubation. Samples from left to right: (a) 0.1 M sodium acetate, pH-2.0, (b) 0.1 M sodium acetate, pH-4.0, (c) 0.1 M sodium phosphate, pH-6.0, (d) 0.1 M sodium phosphate , pH-7.2, (e) 0.1 M HEPES, pH-8.0, (f) 0.1 M HEPES, pH- 9.0, and (g) sodium borate, pH-11.0. B) ThT fluorescence at a variety of temperatures, after 24 h incubation. Samples from left to right: (a) -20°C, (b) 4°C, (c) 22°C, (d) 37°C, (e) 60°C, and (f) 80°C. Fluorescence values have all had the appropriate control value subtracted, and are represented as % decrease in fluorescence compared to the control sample. Error bars represent the SD of three replicates.
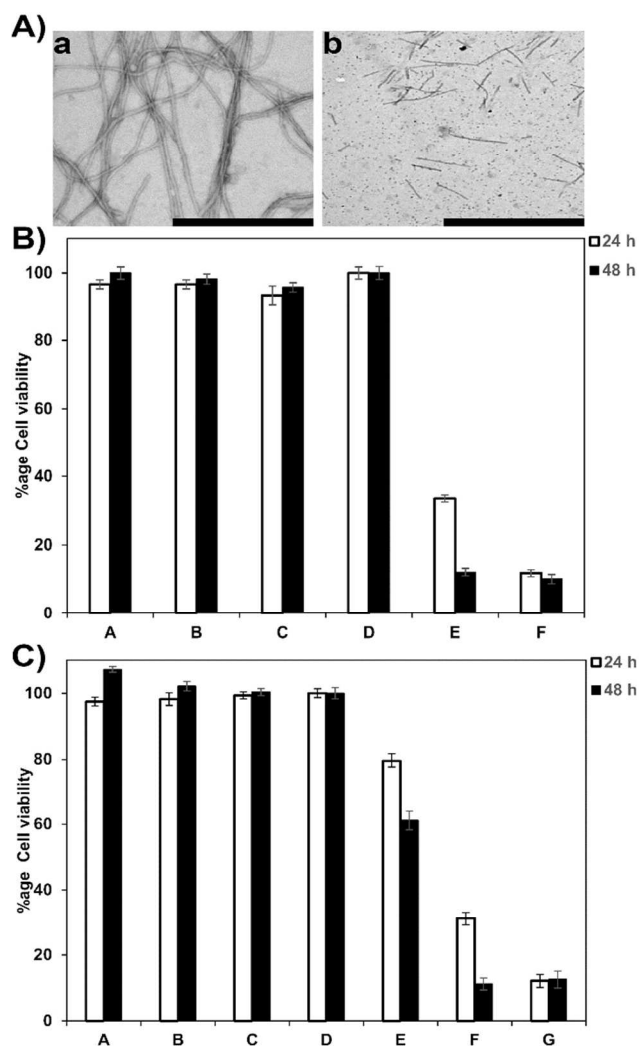
Figure 4. A) Representative TEM images of crystallin PNFs: (a) mature fibrils and (b) fragmented fibrils. Scale bar is 100 nm. B) Hec 1a cell viability, in presence of (a) mature fibrils and (b) fragmented fibrils, (c) crude crystallin protein (10mg/ml), (d) control- nutrient medium + PBS, (e) 10% DMSO, and (f) no-cell sample. C) Hec 1a cell viability, in presence of (a) mature fibrils, (b) fragmented fibrils, (c) crude crystallin protein (10 mg/ml), (d) control- nutrient medium + PBS, (e) control- starvation medium + PBS, (f) 10% DMSO, and (g) no-cell sample. Cell viability is represented as % decrease/increase in number of cells as compared to control (d), nutrient medium is set to 100 %. Error bars represent the SD of three replicates. White columns 24 hours, black columns 48 hours.
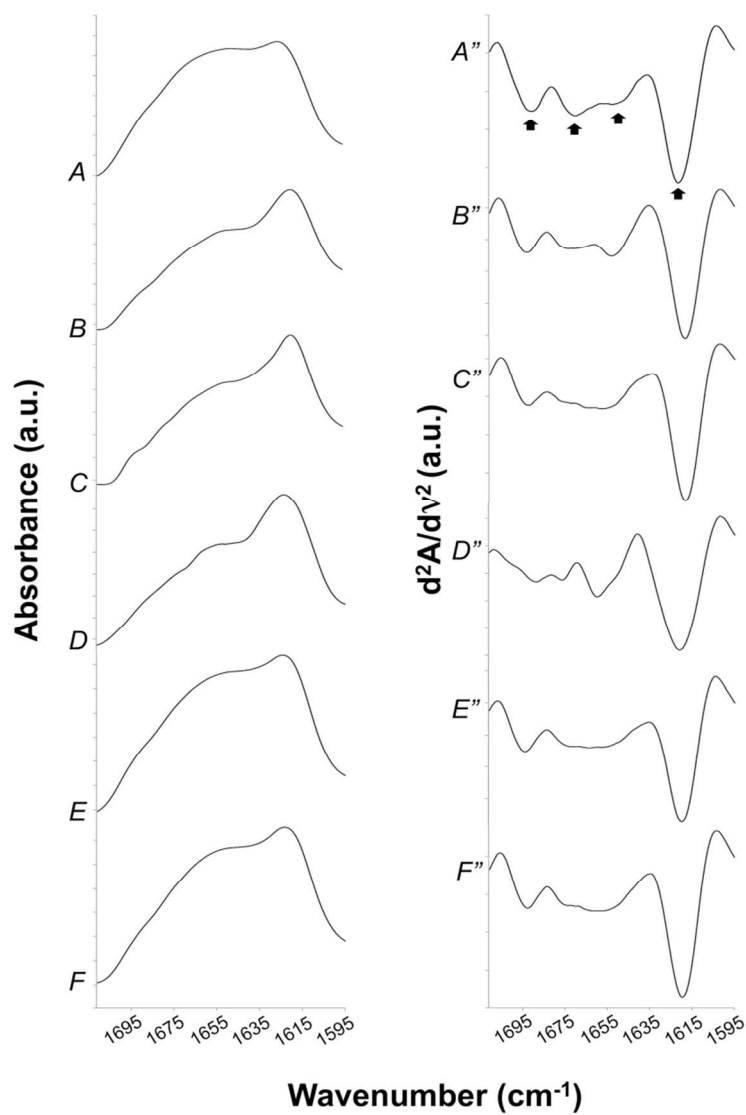
Figure 5. IR absorbance spectra (A, B, C, D, E, F) and 2nd derivative spectra d^2A/dv^2 (A", B", C", D", E", F") of crystallin amyloid nanofibril samples after long-term storage with periods of A) 37, B) 27, C) 13, D) 5, E) 2 and F) 0 months.

Table 1. IRM amide I vibrations of aged crystallin fibrils (wavenumbers taken from minima in second derivatives of IRM spectra) and corresponding secondary structures.

Crystallin PNF age (months)	Antiparallel β-sheet (cm⁻¹)	Random coil (cm⁻¹)	Turn (cm⁻¹)	Antiparallel β-sheet (cm⁻¹)
0	1619	1655	1662, 1676	1693
2	1620	1650	1663, 1670	1693
5	1620	1650	1660, 1676	1689
13	1618	1656	1664, 1675	1693
27	1618	1652	1672	1693
37	1621	1652	1670	1692

Nanoscale Accepted Manuscript